Int J Adv Manuf Technol (2009) 44:223–237
DOI 10.1007/s00170-008-1822-9

ORIGINAL ARTICLE

Investigation of the effects of main roll-forming process parameters on quality for a V-section profile from AHSS

John Paralikas · Konstantinos Salonitis · George Chryssolouris

Received: 19 May 2008 / Accepted: 27 October 2008 / Published online: 19 November 2008

Abstract The cold-roll-forming process is one of the main processes for mass production of the profiles with constant cross-section in many industrial sectors. The introduction of advanced high-strength steels (AHSS), such as DP-series and TRIP-series, into the production of roll-formed profiles has brought new challenges. The current paper exploits the finite elements (FE) method and investigates the effects of the main roll-forming process parameters, namely the roll-forming line velocity, rolls inter-distance, rolls gap, and rolls diameter, on quality characteristics. These characteristics are the distribution of longitudinal and transversal strains on final profile, total, and elastic longitudinal strains and longitudinal residual strains at strips edge along the forming direction and dimensional accuracy of the profile after the final roll station.

Keywords Cold roll forming · Modeling · AHSS · Longitudinal strains · Residual strains · Dimensional accuracy

1 Introduction

Cold roll forming is a continuous bending operation, during which a long strip of metal is passed through consecutive sets of rolls or stands, each performing only an incremental part of the bend, until the desired cross-section profile has been obtained [1–4]. The introduction of advance high-strength steels (AHSS) into the production of roll-formed profiles has accentuated existing processing problems and brought new challenges. These problems include defects in production and limitations in surface quality and dimensional accuracy. The principal difference of AHSS from conventional steel lies in their microstructure [5]. They combine higher yield strength with lower total elongation. This imposes the challenge for higher loads on the rolls during roll forming, as well as for a greater impact on defects and springback issues. Any defects caused during the roll-forming process could be bow, camber, twist, edge wave, corner buckling as well as edge cracking, and splitting. These kinds of defects and quality characteristics are mainly affected by various types of deformations, namely, the transversal elongation and bending, longitudinal elongation and bending as well as the shear in strip's plane and thickness direction [6]. The only desirable deformation for the bending of the profile is the transversal bending, while the others are characterized as redundant deformations and are responsible for the existence of main defects during the roll-forming process.

The scope of the current study is to provide an adequate model, exploiting numerical simulation, for the prediction and investigation of the effect of main process parameters on redundant deformation in the roll forming of AHSS materials and consequently on defects. Main redundant deformations that would be investigated on the V-section are longitudinal strains at strip edge, the distribution of longitudinal and transversal elongations at the final profile, as well as geometrical distortions in the final profile after the final roll station.

The amount of these redundant deformations could become a metric for the control and measurement of specified tolerances from the customer and the desired product's quality characteristics (elimination of defects) [2]. Numerical simulation is used for the prediction of the

J. Paralikas · K. Salonitis · G. Chryssolouris (✉)
Laboratory for Manufacturing Systems and Automation,
Department of Mechanical Engineering and Aeronautics,
University of Patras,
Patras 265 00, Greece
e-mail: xrisol@mech.upatras.gr

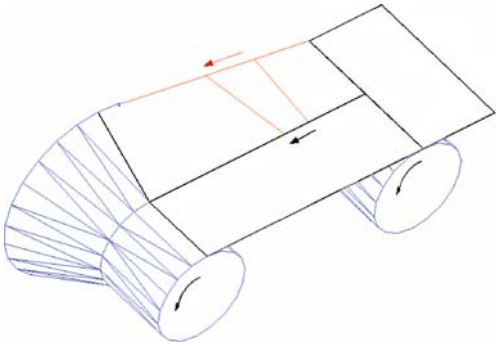

Fig. 1 Flange travels greater distance than web through successive rollers (top rolls are not shown)

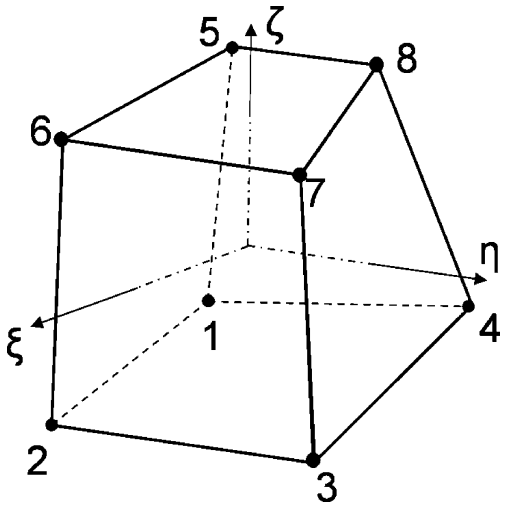

Fig. 3 Eight-node solid hexahedron element [19]

amount of these deformations at specific points of the cross-section. The influence of main process parameters, such as line velocity, roll stations inter-distance, roll gap, rolls diameter, existence of lubricants (friction coefficient), and strip thickness is investigated. As a result, this study could become a guideline for tooling designers for a quick and optimum design and set-up of a roll-forming line. Moreover, the prediction of redundant deformations can prevent defects from happening before the production starts and significant costs savings to occur [3].

In addition, both the application of guidelines and the combination of the optimum process parameters can lead the quality characteristics of the final roll-formed product to be improved. This improved design and set-up of the roll-forming line could be compared with the conventional case, and the reduction of redundant deformations to be benchmarked.

During roll forming, the material in the flange travels a greater distance through successive rollers, as shown in Fig. 1. Thus, a longitudinal elongation is created at the edge of the flange. This causes longitudinal strain in the flange, which should not enter into plastic region in order for large longitudinal residual stresses in the finished profile to be avoided [7]. These residual stresses are responsible for any major defects, such as camber, bow, and twist. The residual strain is the difference between the maximum longitudinal strain and the longitudinal strain at the roll exit. The higher the residual strain is, the higher the defect rate of the finished product becomes [8].

Specific tolerances and quality standards could be set for the production of the V-section. Tolerances, specified by the customer, the product designer, and the roll designer, affect the roll design as well as the number of roll stations required. Tighter tolerances require more roll stations [6]. Consequently, the tooling cost increases and affects the product's cost. Dimensional cross-sectional tolerances from ±0.25 mm to ±0.78 mm (±0.010 to ±0.031″), as well as angular tolerances of ±1° can be achieved with roll-forming equipment [4]. Moreover, tolerances are affected by the method of the roll forming, such as pre-cut or cut-at length or the post-cut method. In the present study, the pre-cut method was chosen, for saving computing effort.

During the previous years, the CAE systems for tooling design used "rules of thumb" for analyzing the roll-forming

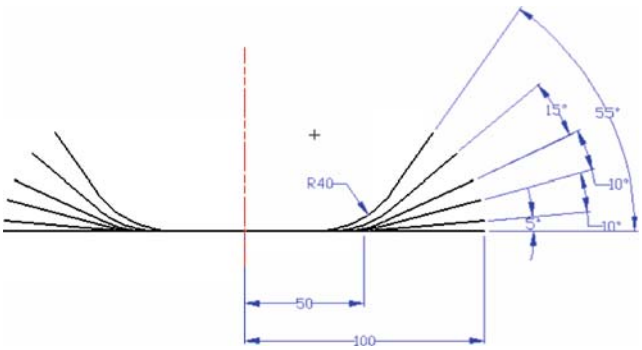

Fig. 2 Flower of the V-section profile (*middle layer*) with symmetry line

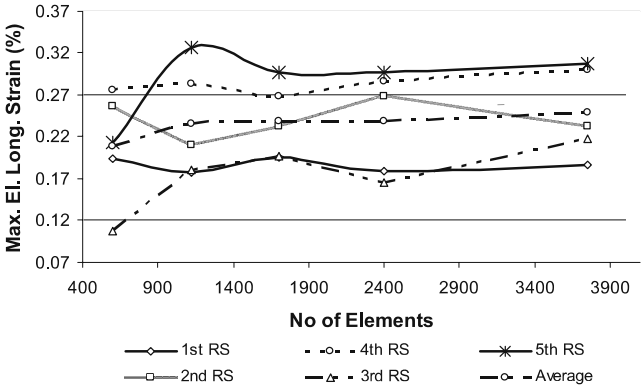

Fig. 4 Maximum longitudinal strain% at each roll station vs. number of strip elements

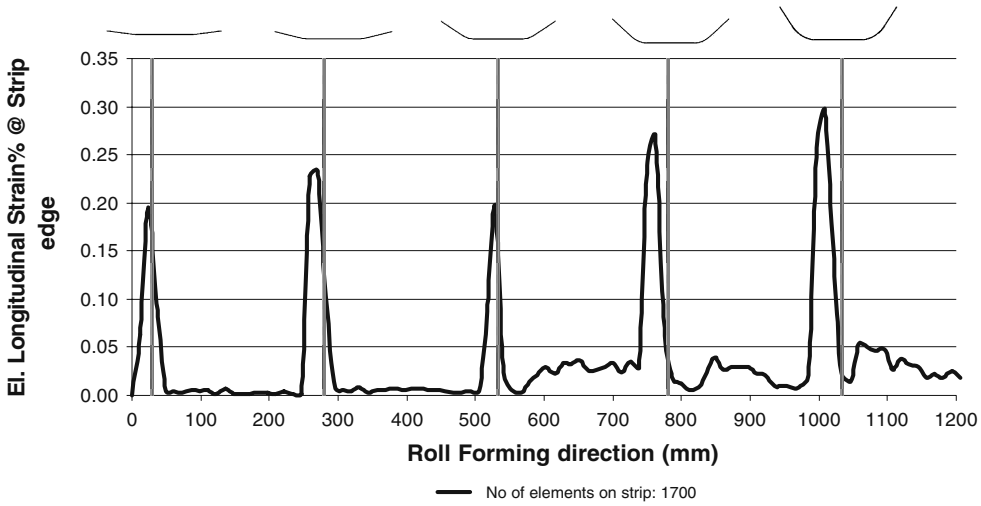

Fig. 5 Longitudinal elastic strains% at strip edge along the roll-forming line direction

process. The FE analysis has been used for validating the design from CAE tools. The disadvantage of the FE analysis is the large demanding CPU time, as special profiles need up to 40 roll-forming stations [7]. Several attempts have been made for defects and redundant deformations to be predicted through simulations using numerical methods of the roll-forming process.

Jeong et al. [9] prepared a model for analyzing and predicting the longitudinal strains and the numerical values of camber and bow of the final product for two different flower patterns. The SCP-1 material model was used and the swift formula was applied $\sigma^f = K(\varepsilon_0 + \varepsilon)^n$. The implicit time integration method and the SHAPE-RF program were used. Bui and Ponthot [10] simulated the cold-roll-forming process, and the results of the longitudinal strains and the displacement trajectories were compared with experimental results available in literature. Parametric study has been performed for material properties, inter-stand distance, roll-sheet friction, and roll velocity. It was concluded that for HSS materials the amount of springback is significant. Bhattacharyya et al. [11] investigated the longitudinal membrane strains when single or multiple roll stations are used. There was a conclusion that the level of the peak strain was dependent on the bend angle increment, and the longitudinal strain increased almost linearly with the increase of this angle increment. Chiang [12] investigated how the flange length and the web width of a U- and V-shaped profile influenced the average peak longitudinal strain at flange. They concluded that the average peak of the longitudinal strain increased almost linearly with the increase of the flange length, but without a significant change during the increase of the web width. Fei-Chin Zan [13] modeled the cold-roll-forming process using explicit dynamic method, in which the rollers were stationary and assumed as being rigid. They examined how the friction forces affected the waviness surface of a Z-profile. The tension stresses applied were greater than the yield limit of the material (365.9 MPa) and the friction coefficient was introduced (0.05/0.1). Zhu et al. [14] investigated the influence of the flange length, material thickness, and bed

Fig. 6 V-section roll-forming model into LS-Dyna

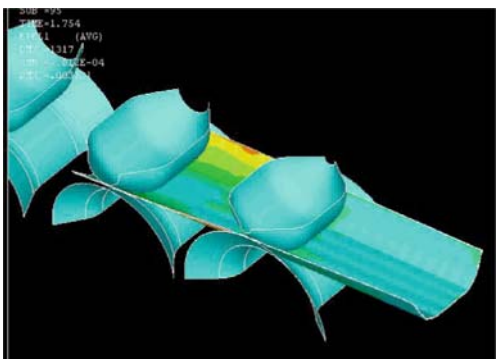

Fig. 7 Contour of longitudinal strains during roll forming of the V-section profile

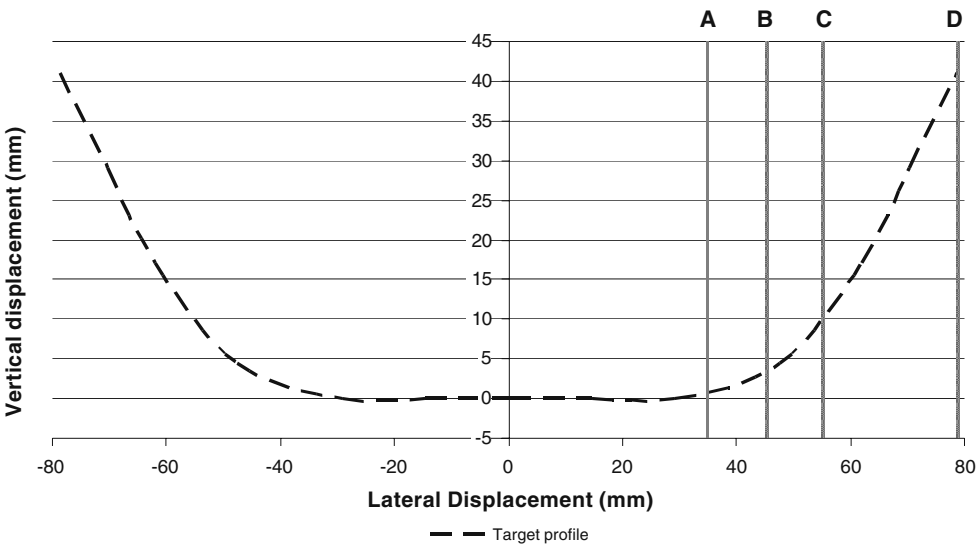

Fig. 8 Target roll-formed profile, and points for observation (*A*, *B*, *C*, and *D*)

angle increment on the longitudinal membrane strain at flange edge. They concluded that the longitudinal strain increased with the increase of the flange length, material thickness, and the bend angle increment. Lindgren [15] created a model for predicting the longitudinal membrane strain in the flange and for analyzing the contact between the tools and the strip, using the MARC/MENTAL FE tool. Lindgren [16] investigated the change in the longitudinal peak membrane strain, at the flange edge, and the deformation length when the yield strength increased. Their results can be used for determining the number of forming steps and the distance between them when designing the cold-roll-forming machine. The result from the simulations shows that the longitudinal peak membrane strain decreases and the deformation length increases when the yield strength is increased. Panton et al. [17] stated that the longitudinal peak strain occurs when the strip is in first contact with the rolls. The peak strain should not enter the plastic region, since the longitudinal plastic strain will give a residual stress that causes defects on the profile as wave edges and longitudinal curvature. Bhattacharyya et al. [18] developed and verified a semi-empirical method for calculating the roll load during the roll-forming process. This method is based on equating the external work with that of the internal bending and stretching and then adding an extra load, due to the longitudinal reverse bending of the beam. Nishikawa et al. [19] proposed an alternative roll-forming method into which a cross-section of the material can be changed gradually. This method integrates a system into which a movable and rotatable roll stand that enables high-speed and continuous roll-forming process. A case study was analyzed for the roof rail of an automotive body-in-white. A single piece roll-formed and stretch-bended beam with non-constant cross-section was compared with two-pieces of stamped and joined parts. The whole technology to be developed was analyzed and the shear forces developed within a plate thickness were discussed. Moen et al. [20] proposed a mechanics-based prediction method of the initial

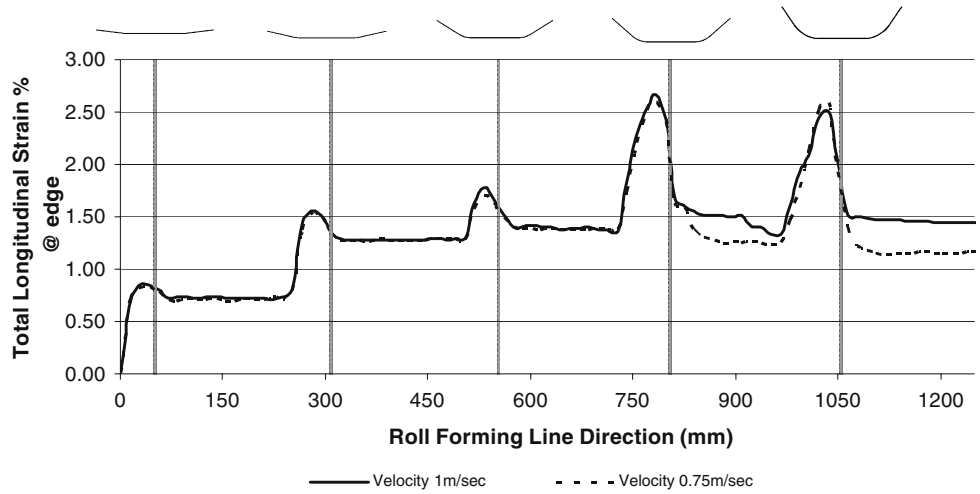

Fig. 9 Total longitudinal strain% at strip edge for different roll-forming line speeds

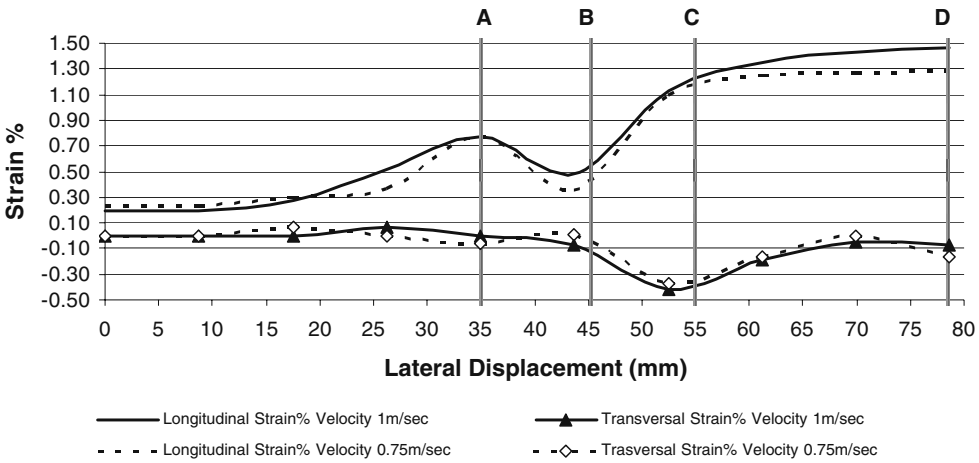

Fig. 10 Longitudinal and transversal strains% distribution on profile for different velocities after the exit from the final roll station

residual stresses, from the coil and effective plastic strains in cold-formed steel members. Steel sheet coiling and roll forming were investigated, with the use of the structural mechanics methods for the calculation and the prediction of the through thickness residual stresses and strains distributions caused from coiling, uncoiling, and flattening of the sheet. Validation of the residual stresses was implemented from experimental results on 18 roll-formed members, and a good agreement emerged. It has been shown that a cold-roll-formed member has both transverse and longitudinal residual stress distributions and the shapes of these distributions are non-linear through the thickness. Heislitz et al. [21] predicted deformed geometry and strains distributions using a commercial FEM code and compared them with results from previous experiments conducted. This study was mainly focused on the procedure of conducting FEM calculations for the roll-forming process and application on the design of a roll-forming process. The adaptive mesh refinement and the half symmetry of the profile were used so as to save CPU time. Longitudinal strains were predicted and compared with experimental results for three points of the strip's flange, and the final profile was predicted after the deformation was completed. Nefussi and Gilormini [22] proposed a kinematic approach for predicting the optimal shape and the deformed length of a metal sheet during the cold-roll-forming process. The middle surface of the strip was described as a Coons patch, and the velocity field has been defined on this surface. The plastic work rate depends only on this geometry parameter, and this parameter's minimization provides the optimal shape of a strain-hardening rigid-plastic material. This method was applied to a simple case, only one roll stand and only one type of a profile. The main drawback of this method is its inability to predict springback, as only the rigid-plastic behavior has been considered. Sheu [23] simulated the cold-roll-forming of a steel process, using FEM code. The blank was pushed through the rollers into the roll-forming machine, and the rollers were running on the fixed-end blank rather than moving the material. Friction conditions were tested so as to approach the experimental results. In order to save calculation time, the working speed was higher

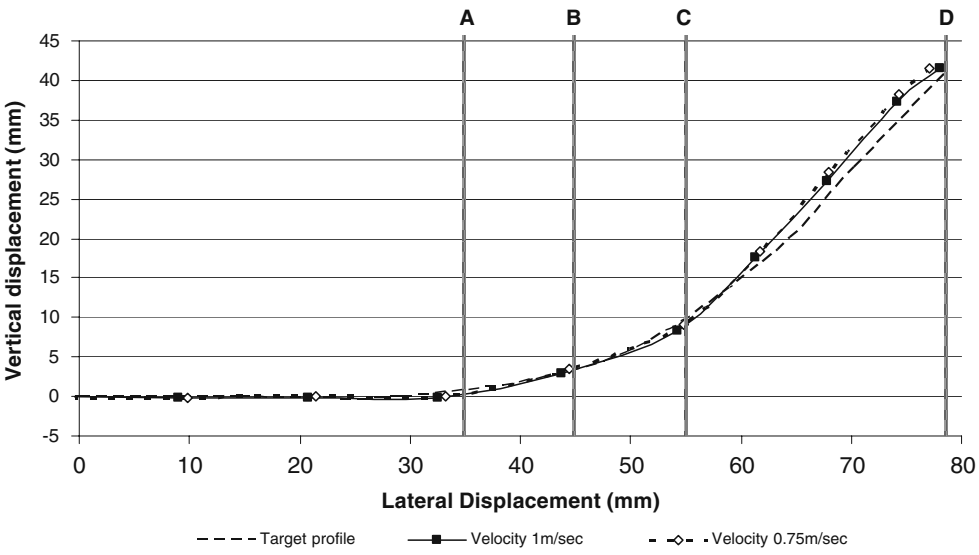

Fig. 11 V-section profile for each velocity after the final roll station

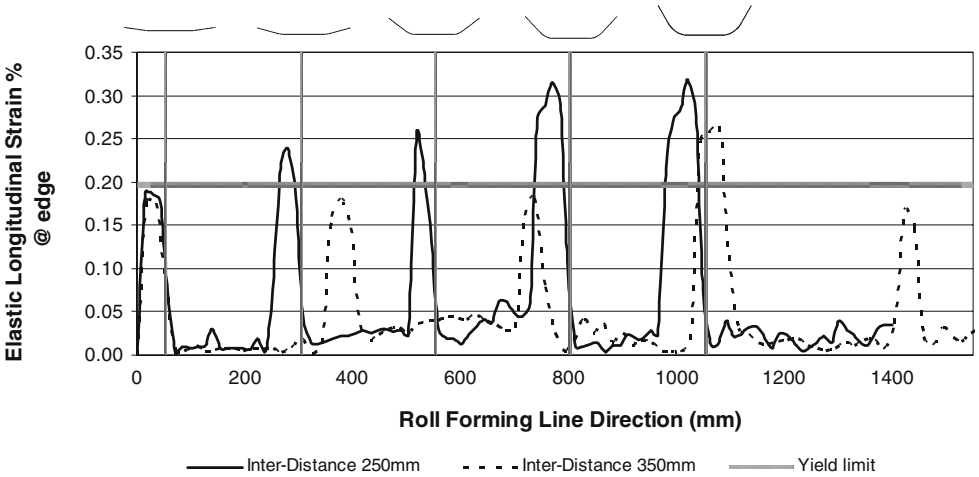

Fig. 12 Elastic longitudinal stain% at flange edge for different roll stations inter-distances

but it still confirmed the experimental results. The results for axial and shear strains were predicted during the bending process of the material. The Taguchi method was adopted in order for an optimum flower diagram to be designed. Hong et al. [24] estimated the forming length of the strip in the roll-forming process taking into consideration some factors such as material properties, strip thickness, roll diameter, roll velocity, and the deformation of the material that influences the forming length. The interaction of factors affecting the forming length was also investigated. Longitudinal strain results were compared with experimental ones. It was concluded that the hardening exponent of the material has a more significant effect on the forming length. Lindgren et al. [25] investigated the roll forming of steel, at larger bending angles, using partial heating of the material itself. This partial heating increases the ductility of the high-strength steel and allows the forming of greater bend angles. Partial heating was applied to cold-rolled TRIP steel. The influence of resistance heating (500–1,200°C) on the material, in the bending area before and after roll forming, has been investigated. It was concluded that partial heating increases the ductility of the materials, but increased heating would cause surface defects. The partially heated material shows three different regions, those of unaffected, transition, and recrystallization, as recrystallization starts in the center and grows with a higher power input.

2 Modeling of roll-forming process

2.1 Geometry and element type

A V-section symmetrical profile was selected for the implementation of the current study, with a total bending angle of 55°. Five roll stations were initially designed for the roll forming of the V-section profile, as the flower of the designed profile can be seen into Fig. 2. For the first roll station, the bend angle was set at 5°, for the next two at 10° and for the final two angles at 15°. Having exploited the symmetry of the profile, only half of it was modeled as the horizontal symmetry line, shown in Fig. 2. This resulted in saving CPU time and allowed faster and more flexible runs of the simulation models.

For modeling the entire roll-forming line and the strip, two different element types were used. SHELL163 elements were used for the rigid rolls, while SOLID164

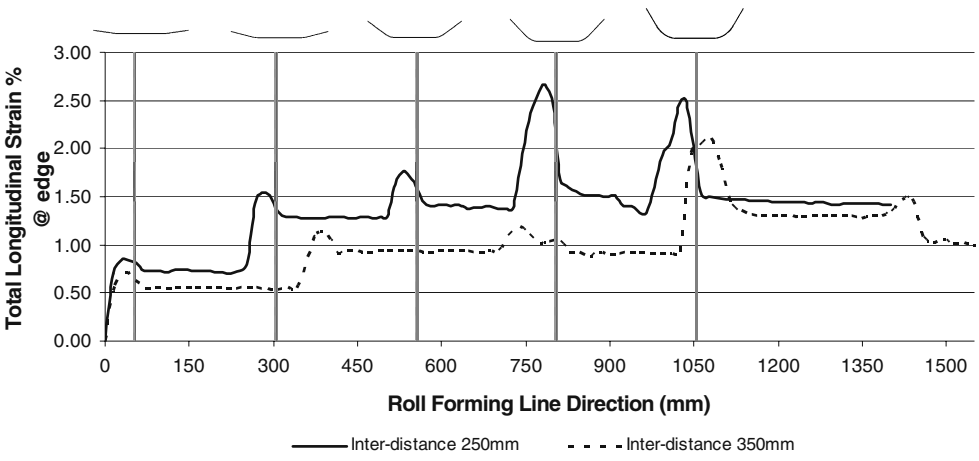

Fig. 13 Total longitudinal strain% at strip edge for different roll stations inter-distances

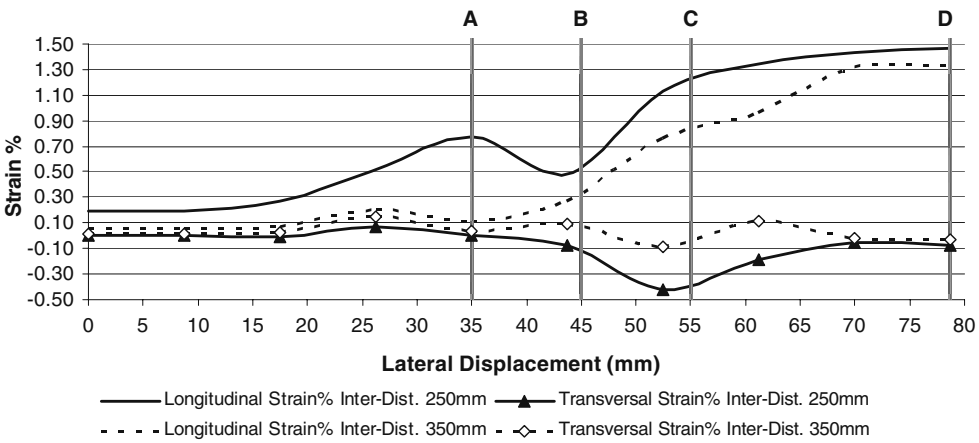

Fig. 14 Longitudinal and transversal strains% distribution on profile for different roll stations inter-distances after the exit from the final roll station

elements were used for the deformable strip. SOLID164 is an eight-node brick element, and it uses reduced integration plus viscous hourglass control for faster element formulation [18, 26, 27] (Fig. 3).

2.2 Material model and meshing

For the material model, the isotropic hardening model was chosen. In this material model, the center of the yield surface is fixed but the radius is a function of the plastic strain [19]. The yield condition for this material model is given by the equation $\sigma_y = \sigma_o + \beta E_\rho \varepsilon_{eff}^p$, where σ_y is the yield stress, σ_o is the initial stress at plastic region, β is the hardening parameter (β=0–1), E_p is the tangent modulus and ε_{ff} is the effective strain. For the rolls, the rigid material model of the Ls-Dyna [27] was chosen, with all rotations and all translations to be constrained. Consequently, the rolls were assumed as stationary (not rotating cylinders) and rigid. Approximation of the effect of the rotating rolls into modeling was the input of the rolling friction coefficient between the rolls and the strip. Concerning the vertical symmetry of the strip, the lateral displacements along the symmetry line were totally constrained. The rotational constrains were also tested along the longitudinal axis, but the results were the same as the first ones. This can be attributed to the fact that no deformation occurs in the symmetry plane, so as to affect the boundary conditions. Thus, only the lateral displacements were constrained in order to save computational time.

The material used in the current study is the AHSS DP600-HDG with 2 mm thickness. DP600-HDG steel has a yield limit of 0.2% at 417 MPa, which corresponds to true strain 0.005087. The hardening parameter of DP600-HDG is 0.136 and the tangent modulus corresponds to 17,500 MPa. For the optimization of the meshing size of the elements on the deformable strip, the meshing convergence procedure was followed, as shown in Fig. 4.

For almost all roll stations, and the average of the maximum longitudinal values, the model seems to be converging for 1,700 elements on the strip and above. It was concluded that for 1,700 elements on the strip and above, the results for the maximum attainable longitudinal elastic strain

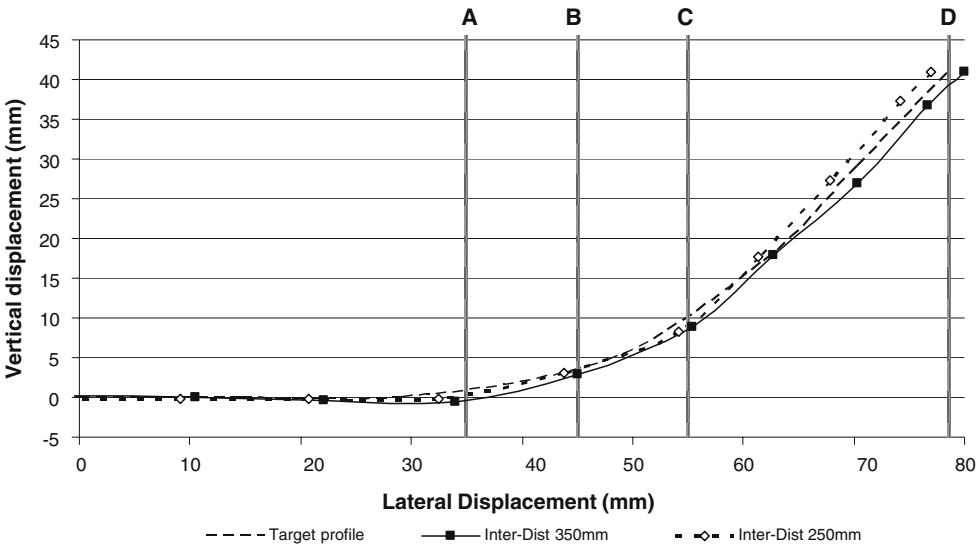

Fig. 15 V-section profile for each inter-distance after the final roll station

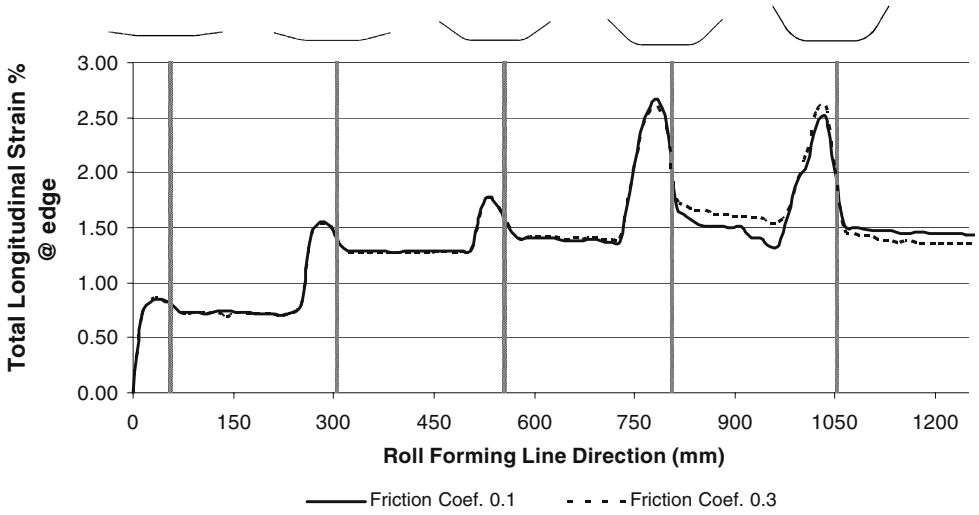

Fig. 16 Total longitudinal strain% at strip edge for different friction coefficients

at each roll station, did not change significantly. Thus, 1,700 elements on the strip were used in the current study. The longitudinal membrane strains were measured in the middle layer of the strip's flange edge, 24 mm away from the strip front edge. This is because the front edge experiences greater deflections due to first hits on the rolls. The elastic longitudinal membrane strains along the roll-forming direction of 1,700 elements on the strip are shown in Fig. 5.

2.3 Contact and loading conditions

For contact option, the single automatic surface was chosen. In this option, all external surfaces of the model were taken into account for contacting. Friction coefficient 0.1 was inserted as default, simulating in this way the presence of the lubricant during roll forming.

Concerning the loading conditions, constant velocity along the roll-forming line direction was imposed on the nodes of the strip. Due to the symmetry of the profile, the half geometry was modeled, as it is shown in Fig. 6. The first roll station is comprised of straight rolls, as no deformation occurs, and it plays the role of the straightener in front of the roll-forming line. This is important to be imported in the model, since it constrains the strip as it enters into the first roll station.

3 Results and discussion

A parametric study was implemented for the most important roll-forming-process parameters. These parameters cover the roll-forming line speed, the roll stations interdistances, the existence of lubricant (friction coefficient), the rolls gap and the rolls diameter.

The results discussed and compared are the total and elastic longitudinal strains at the strip's edge along the roll-forming direction, as well as the distribution of longitudinal and transversal strains on the profile after exiting the final roll station. In conclusion, the final produced profile, from the roll-forming line, has been compared with the target designed profile from the flower. The springback is assumed not to be affected from the selected parameters. In the bending operations, the springback is influenced from the geometry, the bending radius, the material properties and the strip

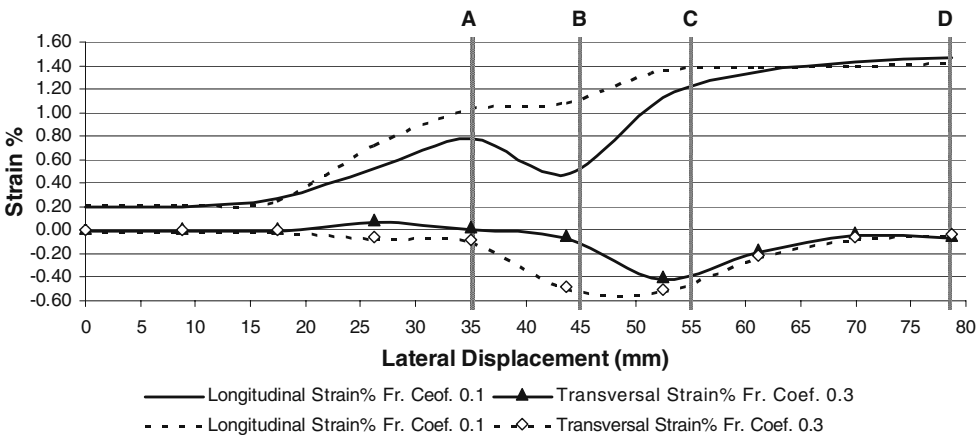

Fig. 17 Longitudinal and transversal strains% distribution on profile for different friction coefficients after the exit from the final roll station

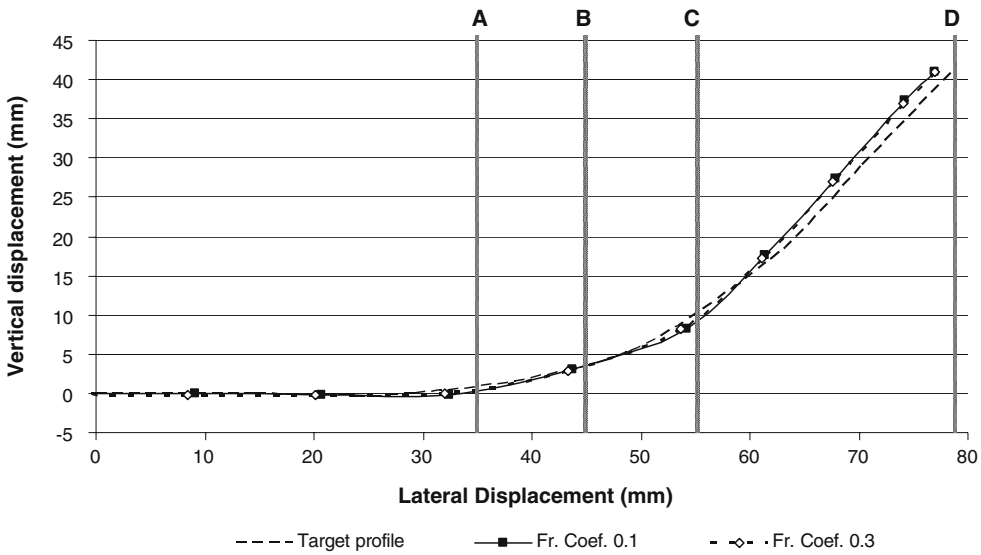

Fig. 18 V-section profile for each friction coefficient after the final roll station

thickness. In the current study, these parameters remain constant, and thus, the springback is not investigated in the final profile. This could be an issue for future studies of the roll-forming-process simulation (Fig. 7).

The final target roll-formed profile can be seen in Fig. 8, in which the points of observation (A, B, C and D) were indicated. These points include the critical ones of the bend radius, as well as the final edge of the V-section profile.

3.1 Roll-forming line velocity

The roll-forming line speed is a major process parameter, as by changing the speed, the productivity of the line is mainly affected. The main objective is to keep the line speed of the machines at a maximum. The current study examines two different line speeds on the V-section profile in order to investigate how this change in speed affects the redundant deformations and consequently, the product's quality.

Two different line speeds were simulated into models for the roll forming of the V-section profile, 0.75 m/s and 1 m/s. These are typical operational speeds used in production lines. Figure 9 compares the total longitudinal strains (%) along the roll-forming direction. This value was taken at strip's edge 24 mm away from the front edge, as at the front edge, there was an extensive distortion, due to the hitting of the strip on the rolls. It is noticeable that the peaks of strains appear before the rolls' centerline, since the contact of the strip with the rolls occurs before the centerline.

The line speed variation mainly affects the residual longitudinal strains at edge, as well as the distribution of the strains along the profile. Increasing the line speed will not primarily affect the peaks, but the total residual strains in a longitudinal direction. As seen from the distribution of strains in Fig. 10, the maximum longitudinal strain occurs at the strip's edge.

Excessive longitudinal strains and the non-uniform transversal distribution of a longitudinal strain can cause longitudinal bow, camber, and twist [6]. The non-uniform distribution of strains is inevitable during roll forming, but the magnitude of the peak could be reduced by reducing the line speed.

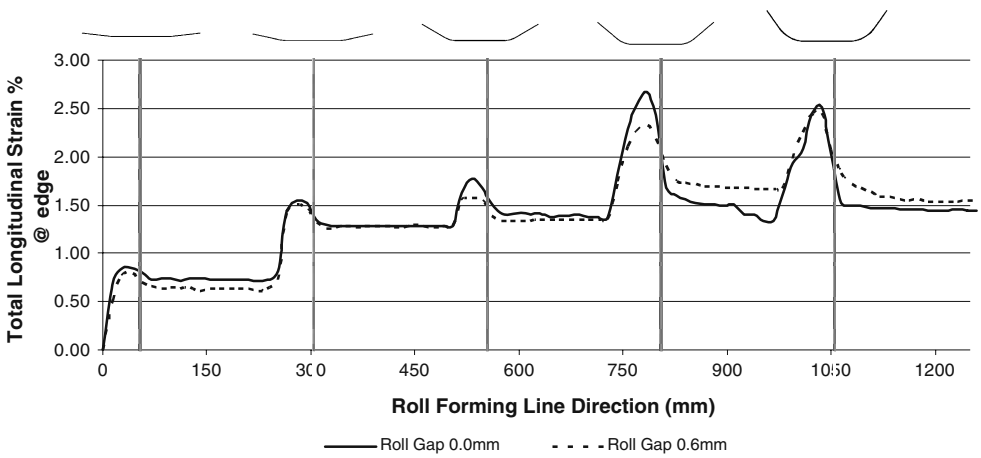

Fig. 19 Total longitudinal strain% at strip edge for different roll gaps

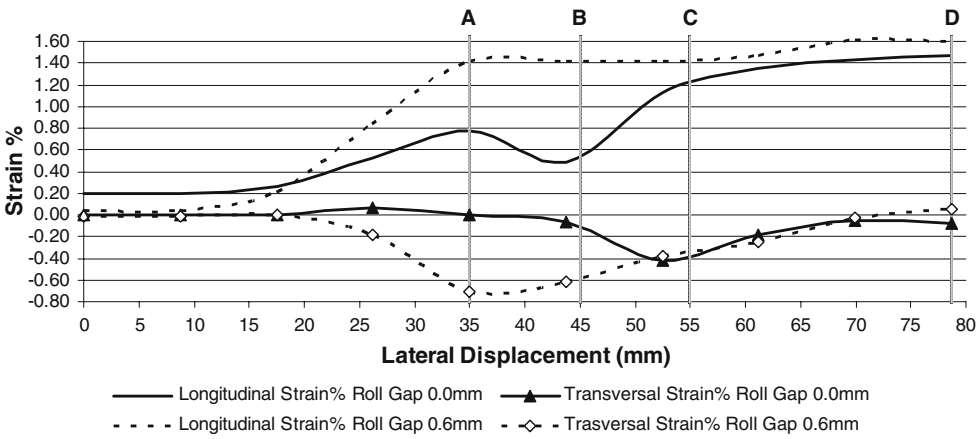

Fig. 20 Longitudinal and transversal strains% distribution on profile for different roll gaps after the exit from the final roll station

The two profiles produced after the exit from the final roll station are shown in Fig. 11. It should be noted here that there was no springback analysis implemented after the exit from the final roll station. The peak of transversal strains before point C leads to extensive distortion at the folding line and loss of accuracy at the ends.

3.2 Roll stations inter-distance

Geometrical considerations play a major role in the roll-forming line set-up and in the prevention of defects and dimensional inaccuracies. Increasing the distance between the roll stations leads to allowing more length for deformation along the sequential bending angles, and more progressive deformation to occur. A disadvantage of increasing the rolls inter-distances could be the increase in the total length of the roll-forming line.

Elastic longitudinal strains at edge should not overcome the yield limit of the material, as this will mean the occurrence of longitudinal residual strain after roll forming. The elastic longitudinal strains along the roll-forming direction are shown in Fig. 12, with the effect of increasing the roll stations' inter-distance from 250 mm to 350 mm.

In Fig. 13, the total strains and the residual ones in longitudinal direction can be observed, where increased inter-distances lead to the higher recovery of strain.

Moreover, the distribution of longitudinal and transversal strains is affected by increasing the rolls' inter-distance. A lower magnitude of peaks and a more uniform distribution can be achieved by increasing the rolls' inter-distance (Fig. 14).

Dimensional accuracy is also affected by the rolls' inter-distances, as the two profiles vary significantly from the target. The two profiles for different inter-distances can be seen in Fig. 15.

3.3 Friction coefficient

Friction exists between the rolls and the sheet during roll forming, as the driving power is transmitted from the rolls

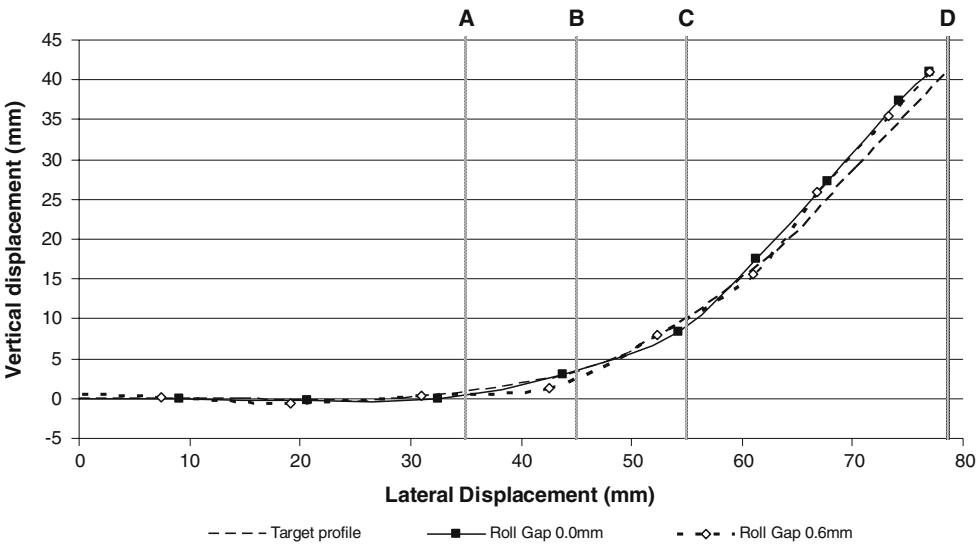

Fig. 21 V-section profile for each roll gap after the final roll station

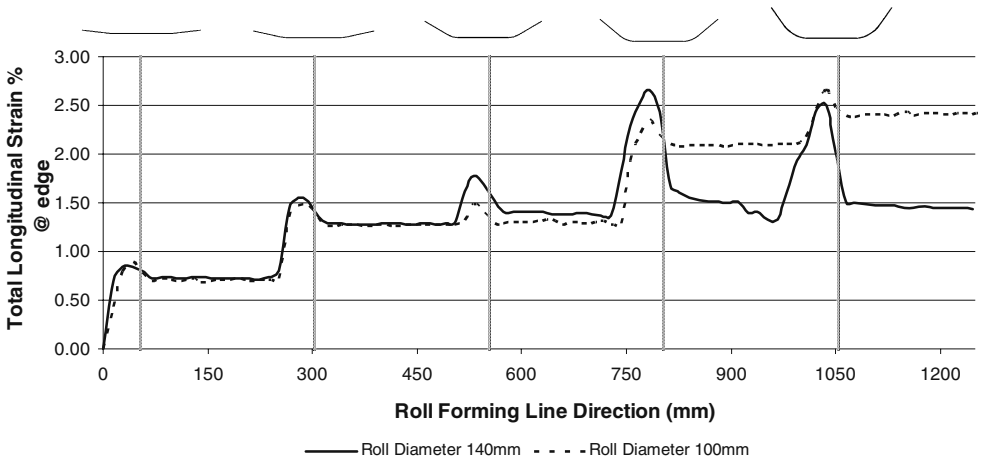

Fig. 22 Total longitudinal strain% at strip edge for different rolls diameter

to the strip [10]. It is generated due to the relative movement between the rolls and the strip, and it is enhanced by the surface speed differential of the rolls [6]. Lubrication is also used during roll forming, because it prevents tools from wear, and dissipates the heat generated due to the forming of thick sheets. There are five lubricant categories for roll forming, namely, evaporative compounds, chemical solutions (synthetics), microemulsions (semisynthetics), macroemulsions (solubles), and petroleum-based lubricants [6]. The selection of the appropriate lubricant is based mainly on the materials and desired characteristics.

In the current study, the effect of different friction coefficients during roll forming is investigated. The effect of different friction coefficients is minor, at smaller bending angles, and at the longitudinal strain peaks along the roll-forming direction. It seems to be mainly affecting the residual longitudinal strain and the distribution of transversal strains along the profile, as shown in Figs. 16 and 17.

The dimensional accuracy of the final produced profile does not seem to be affected by the different coefficients, since there are no dimensional changes in the V-section profiles as it is shown in Fig. 18.

3.4 Roll gap

Roll gap is the clearance between the rolls and the strip, as the latter passes through the former. It is measured in vertical displacement of the clearance on the web, as rolls are designed with the use of the top rolls relief method. This method implies that the upper rolls are not always in contact with the deformable strip on the flange; as there is surface speed differential along different roll diameters.

In this study, the "tight" (0.0 mm) and the "loose" (0.6 mm) roll gaps are investigated. These values are also typical for the industrial practice. There seems to be a difference in the strain peaks, at greater bending angles, as well as in the residual longitudinal strains at the end of the line, as shown in Fig. 19.

The different roll gaps also affect the distribution of the longitudinal and transversal strains along the final profile. Significant is the increase of the transversal strain at the start of the bend (point A), as shown in Fig. 20.

The dimensional accuracy is affected by increasing the roll gap mainly on the bending radius, as excessive transversal strains can cause defects on that area, as shown in Fig. 21.

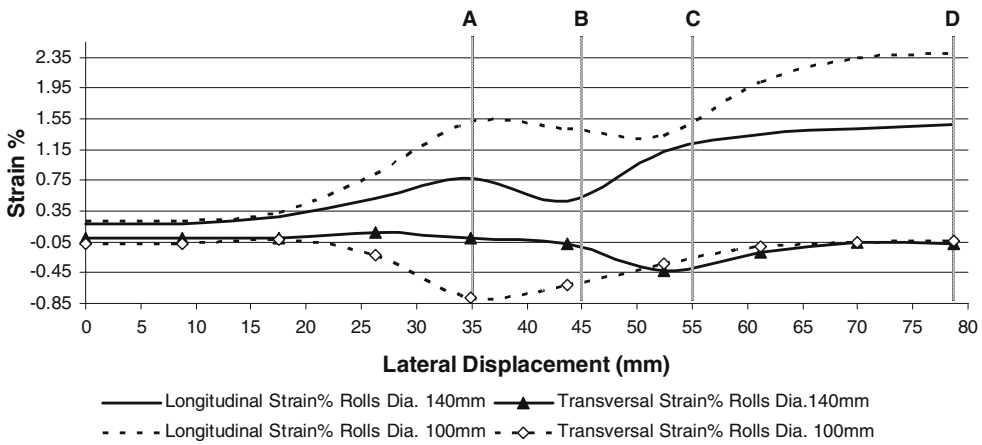

Fig. 23 Longitudinal and transversal strains% distribution on profile for different rolls diameter after the exit from the final roll station

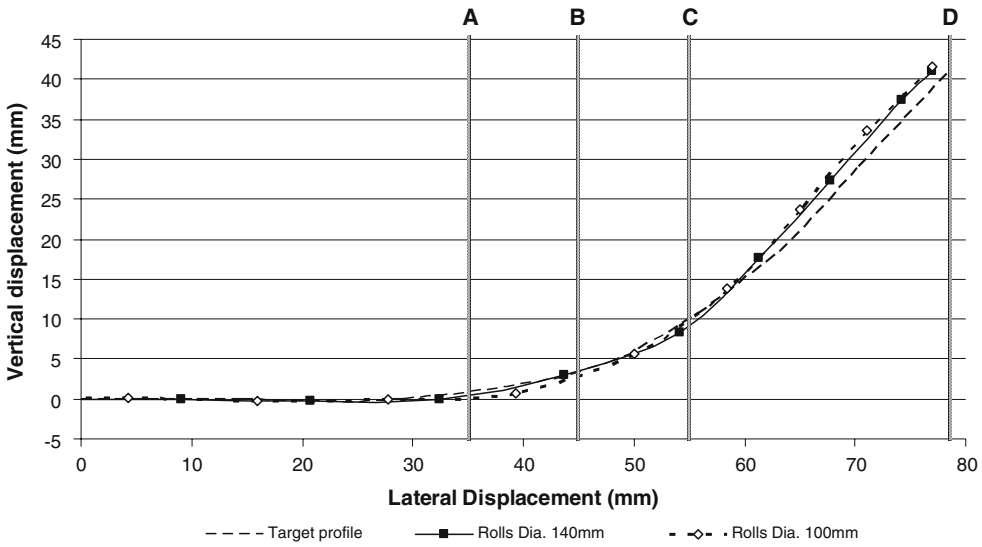

Fig. 24 V-section profile for each rolls diameter after the final roll station

3.5 Rolls' diameter

The selection of the rolls' diameter is affected by numerous factors, namely, the roll-forming machine dimensions, the material to be formed, the section depth, the rolls surface speed, etc. The roll diameter plays a major role in the accumulation of the longitudinal plastic strain on the strip edge along the successive roll stations. Rolls are made by increasing the diameter from one roll station to the other, so as to permit the surface speed to be increased. This is referred to as "step-up" [4]. The speed differential between passes creates a tension in the section material and eliminates the possibility of overfeeding between passes.

In the current study, two different diameters were investigated in the simulation of the roll-forming line of a V-section. As mentioned above, by decreasing the roll diameter, there is an accumulation of the longitudinal plastic strain on the edge of the strip. This is stored onto the strip and exists as residual strain after the roll-forming process. As it can be seen in Fig. 22, by increasing the rolls' diameter, the residual longitudinal strain is reduced.

Moreover, the distribution of the longitudinal and transversal strains at the final profile produced is affected by the alternation of the roll diameter, as shown in Fig. 23.

The excessive transversal strain at point A can cause a twist on the bending line of the produced profile, as shown

Table 1 A synopsis on the effects of main roll-forming process parameters on longitudinal, transversal strains and dimensional accuracy of the profile after the final roll station

Effect on / Increase of	Long/nal strain peak @ strip edge	Long/nal residual strain @ strip edge	Dimensional accuracy	Transversal strain @ bending corner
Line velocity	😐	☹	😐	☹
Rolls inter-distance	🙂	🙂	😐	🙂
Friction coefficient	😐	☹	😐	☹
Rolls gap	🙂	☹	☹	☹
Rolls diameter	😐	🙂	🙂	🙂

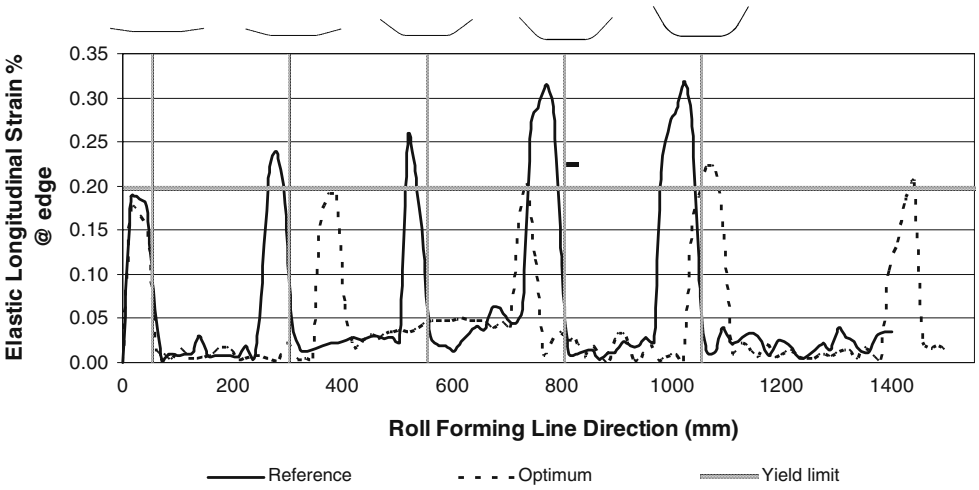

Fig. 25 Elastic longitudinal strain% at strip edge for reference and optimum case

in Fig. 24. This distortion in the bend line also causes dimensional inaccuracies at the profile's legends.

4 Discussion and conclusions

The modeling of the roll forming of a V-section profile has been presented in the current study. The scope of this modeling was to predict longitudinal and transversal elongations, which are not desired during roll forming, at the strip's edge and bending zone. The maximum magnitude and distribution of longitudinal strain, along the profile produced, plays a major role in the present defect and in the dimensional inaccuracies of the profile. In this study, no springback analysis has been investigated on the final profile. The comparison of the profiles has been made by using the same AHSS material (DP600-HGD).

Moreover, the residual longitudinal strains on the strip's edge not only do they affect the quality of the final roll-formed product, but also the post-forming operations, namely welding, cutting, trimming, drilling, etc. These residual strains could affect other post-operations in other manufacturing lines, such as post-stamping of roll-formed beams.

In the current study, the prediction and effects of redundant deformations on the main roll-forming-process parameters were obtained. A summary of these effects on the process parameters can be seen in Table 1.

Based on the results of the parameters in the roll-forming process, the combined effect of these parameters for improving the quality characteristics has been studied. Velocity has been set to 0.75 m/s (reference velocity 1 m/s), rolls inter-distance to 350 mm (reference inter-distance 250 mm), friction coefficient to 0.1, and rolls diameter to 140 mm and thickness remains to 1 mm.

The results of the elastic and total longitudinal strains (%), as shown in Figs. 25 and 26, on the strip edge, show that elastic elongation is under the yield limit in almost all the roll stations. This improved configuration also leads to a reduced accumulation of the plastic longitudinal elongation on the strip edge, where it is at maximum magnitude.

Moreover, the distribution of longitudinal and transversal strains of the V-section profile, after the exit of the final roll,

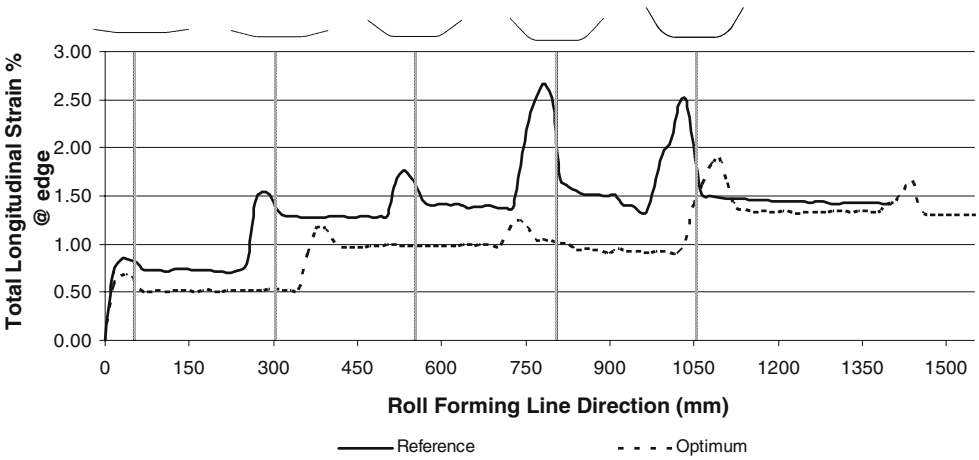

Fig. 26 Total longitudinal strain% at strip edge for reference and optimum case

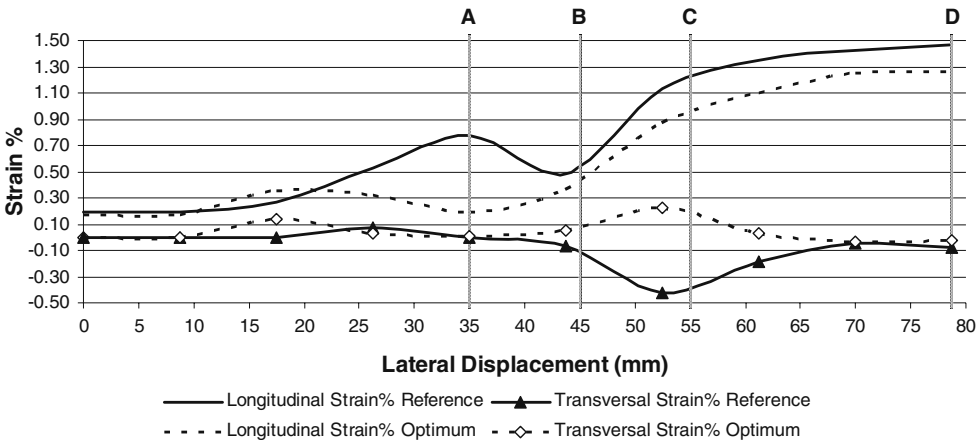

Fig. 27 Longitudinal and transversal strains% distribution on profile for reference and optimum case after the exit from the final roll station

indicates this improvement against the reference case. In almost all points of the profile, the magnitude of longitudinal strains is lower with the use of the improved configuration of process parameters, as shown into Fig. 27.

Regarding the transversal strain distribution over the final profile, it shows an alternation from compression to elongation in a corner bend. Maximum magnitude of the transversal strain is shown to be at the same point of the final profile. This could be a result of the increased roll gap in the corner region of the profile. In addition to that, the dimensional accuracy of the profile has not been affected a great deal. Increased roll gap leads to dimensional inaccuracies on the web and to the corner region of the profile, as shown in Fig. 28. This can also affect the dimensional accuracy of the strip edge's position at point D.

Further study could be done for influencing the parameters affecting the product design, such as material type, width of flange and web, material type, maximum profile height, etc., on redundant deformations and the distribution of them on the profile. Furthermore, an optimization of process parameters could be implemented for the reduction of these redundant deformations and the uniform longitudinal and transversal elongations on the roll-formed product.

Springback analysis could be also incorporated into this analysis, as springback is mainly affected from the radius of the corner, strip thickness, yield strength and elastic modulus of the material [5]. Process parameters that have been studied do not affect mainly the springback of the roll-formed profile and the same material (DP600) has been used for all the models.

Furthermore, the effect of the residual strains in longitudinal and transversal directions from roll forming could be investigated into the stamping process and crash analysis (safety) of the roll-formed products. The complete virtual manufacturing chain for the production of the roll-formed product could be implemented by passing on residual strains from one step to another.

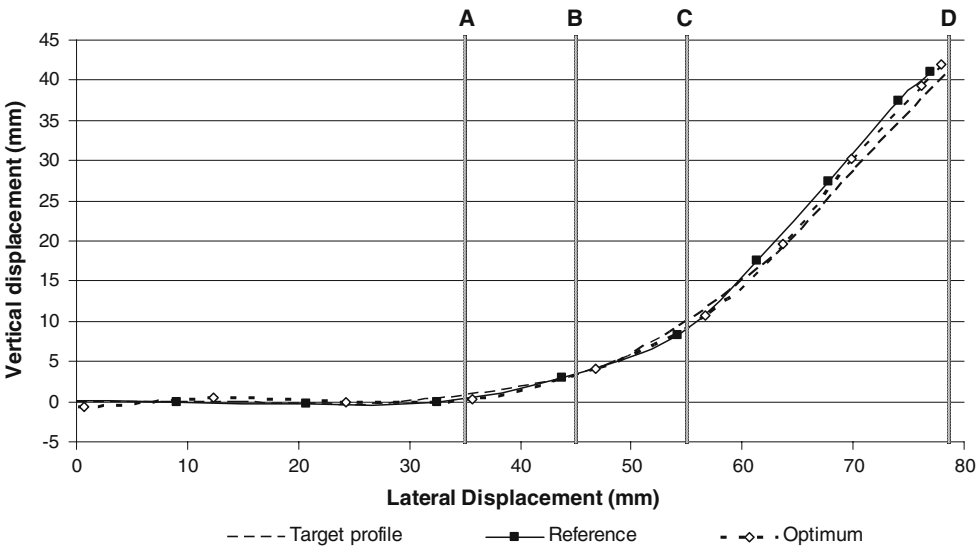

Fig. 28 V-section profile for reference and optimum case after the final roll station

Acknowledgment The work reported in this paper was partially supported by CEC/FP6 NMP Programme, "Integration Multi-functional materials and related production technologies integrated into the Automotive Industry of the future—FUTURA" (FP6-2004-NMP-NI-4-026621)".

References

1. Chryssolouris G (2005) Manufacturing systems-theory and practice, 2nd edn. Springer
2. Salonitis K, Stavropoulos P, Paralikas J, Chryssolouris G (2007) Modeling of cold roll forming process: a preliminary theoretical investigation, Proceedings of the IFAC Workshop on manufacturing modelling, management and control. Budapest, Hungary, pp 211–216
3. Salonitis K, Paralikas J, Chryssolouris G (2008) Roll forming of AHSS: Numerical simulation and investigation of effects of main process parameters on quality, Proceedings of the International Conference of Engineering Against Fracture, University of Patras, Greece
4. Wick C, Benedict J, Veilleux R (1984) Tool and manufacturing engineers handbook, Volume 2 Forming, SME
5. International Iron & Steel Institute (2006) Advanced High Strength Steel (AHSS) application guidelines. Committee on Automotive applications
6. Halmos GT (2006) Roll forming handbook. CRC
7. Lindgren M (2005) Modeling and simulation of the roll forming process, Licentiate thesis, Lulea University of technology
8. Kim YY (2002) Buckling analysis and buckling limit of strain on roll forming process. Thesis of Degree of M.Sc. Sogang University
9. Jeong SH, Lee SH, Kim GB, Seo HJ, Kim TH (2008) Computer simulation of U-channel for under-rail roll forming using rigid plastic finite element methods. J Mater Process Tech. doi:10.1016/j.jmatprotec.2007.11.130
10. Bui QV, Ponthot JP (2007) Numerical simulation of cold roll-forming processes. J Mater Process Tech. doi:10.1016/j.jmatprotec.2007.08.073
11. Bhattacharyya D, Smith PD, Yee CH, Collins IF (1984) The prediction of deformation length in cold roll forming. J Mech Work Technol 9:181–191
12. Chiang KF (1984) Cold roll forming, ME. Thesis, University of Auckland
13. Fei-Chin Zan (2000) Simulation of cold roll forming process, Thesis, University of Pittsburgh
14. Zhu SD, Panton SM, Duncan JL (1996) The effects of geometric variables in roll forming a channel section. Proc Inst Mech Eng 210:127–134
15. Lindgren M (2005) Finite element model of roll forming of a U-channel profile. Dalarna University of Sweden
16. Lindgren M (2007), Cold roll forming of a U-channel made of high strength steel. J Mater Process Tech. doi:10.1016/j.jmatprotec.2006.12.017
17. Panton SM, Zhu SD, Duncan JL (2006) Geometric constraints on the forming path in roll forming channel sections. Proc Inst Mech Eng 206
18. Bhattacharyya D, Smith PD, Thadakamalla SK, Collins JF (1987) The prediction of roll load in cold roll forming. J Mech Work Tech 14:363–379
19. Nishikawa N, Kohama T, Uchino R, Horino K (1997) Development of roll forming technology with gradual cross sectional change, SAE technical paper series 971741
20. Moen CD, Igusa T, Schafer BW (2008) Prediction of the residual stresses and strains in cold-formed steel members. Thin-walled Struct 46:1274–1289
21. Heislitz F, Livatyali H, Ahmetoglu MA, Kinzel GL, Altan T (1996) Simulation of roll forming process with the 3D FEM code PAM-STAMP. J Mater Process Technol 59:59–67
22. Nefussi G, Gilormini P (1993) A simplified method for the simulation of cold roll forming. Int J Mech Sci 10:867–878
23. Sheu JJ (2004) Simulation and optimization of the cold roll forming process, Materials processing and design: Modeling, Simulation and Applications, Proceedings of the 8th International Conference on Numerical Methods in Industrial Forming Processes; doi:10.1063/1.1766566
24. Hong S, Lee S, Kim S (2001) A parametric study on forming length in roll forming. J Mater Process Technol 113:774–778
25. Lindgren M, Bexell U, Wikstrom L (2007) Roll forming of partially heated cold rolled stainless steel. J Mater Process Technol. doi:10.1016/j.jmatprotec.2008.07.041
26. ANSYS Release 10.0 (2005) ANSYS LS-Dyna User Guide, ANSYS Inc.
27. Hallquist JO (2006) LS-Dyna Theory manual, Livermore Software Technology Corp